Schwinger representation approach to the Lipkin model

2006 J. Phys. A: Math. Gen. 39 12457

(http://iopscience.iop.org/0305-4470/39/40/012)

INSTITUTE OF PHYSICS PUBLISHING JOURNAL OF PHYSICS A: MATHEMATICAL AND GENERAL

J. Phys. A: Math. Gen. **39** (2006) 12457–12468 doi:10.1088/0305-4470/39/40/012

Schwinger representation approach to the Lipkin model

Masatoshi Yamamura[1], Constança Providência[2], João da Providência[2], Seiya Nishiyama[2], Flávio Cordeiro[2] and Yasuhiko Tsue[3]

[1] Faculty of Engineering, Kansai University, Suita 564-8680, Japan
[2] Centro de Física Teórica, Universidade de Coimbra, 3000 Coimbra, Portugal
[3] Physics Division, Faculty of Science, Kochi University, Kochi 780-8520, Japan

Received 13 June 2006, in final form 9 August 2006
Published 19 September 2006
Online at stacks.iop.org/JPhysA/39/12457

Abstract

The Schwinger representation and the Marumori–Yamamura–Tokunaga boson expansion are used to describe the Lipkin model in terms of generalized coherent states. The groundstate, first excited state and RPA energies are obtained within several variant types of coherent states. It has been found that generalized coherent states defined in consonance with the parity symmetry of the model describe particularly well the transition from weak to strong coupling, providing a remarkable improvement of the mean-field description of the transition zone.

PACS number: 02.20.Sv

1. Introduction

The Lipkin model was originally proposed by Lipkin, Meshkov and Glick [1] and has been widely used to test several kinds of many-body theories of strongly interacting fermion systems, as, for instance, the Hartree–Fock (HF) and the time-dependent Hartree–Fock (TDHF) methods [2, 3], collective dynamics of many-fermion systems [4, 5], phase transitions and symmetry breaking [6], statistical mechanics of quantum spin systems [7], spin tunnel effect [8], Bose–Einstein condensation [9], quantum entanglement [10], etc. The important issue of the thermodynamic limit of this model has been discussed in [11]. It is defined as a two-levels system in a fixed shell-model potential, the levels having the same j value, one of the levels being just below and the other just above the Fermi energy. Here, j denotes the single-particle total angular momentum, arising from coupling the orbital angular momentum l with the spin angular momentum $s = 1/2$. In the reference state, relative to which elementary excitations are referred and correlations are assessed, the lower level is filled with $2j + 1$ fermions and the upper level is empty. Each magnetic quantum number m, $-j \leqslant m \leqslant j$, is occupied either in the lower level or in the upper level, so that fermions jump, to and from, between the two

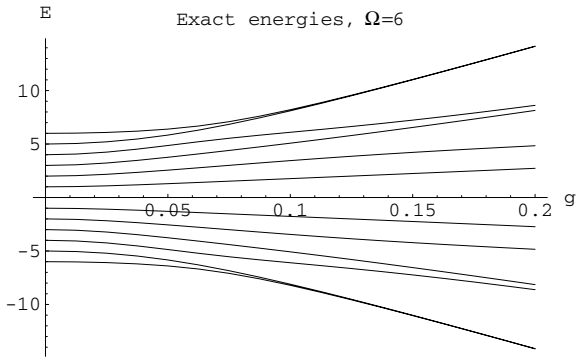

Figure 1. Exact results, showing the energy spectrum as function of the strength g. Notice that, as g increases, the second level approaches the first one and the fourth level approaches the third one. This is a manifestation of the tunnel effect associated with the phase transition. The line $E = 0$ is one of the curves.

levels, preserving the m value. The Lipkin model is a $su(2)$ algebraic model, which means that its Hamiltonian is expressed in terms of the generators of the $su(2)$ algebra realized as appropriate bilinear forms of fermion annihilation and creation operators, a structure which renders the model amenable to an exact treatment and makes it suitable to test theories and approximation methods. The model and some of its applications are reviewed in [6, 12]. A typical spectrum of the Lipkin model Hamiltonian is represented in figure 1 as a function of the coupling constant, showing a clear manifestation of the phase transition exhibited by the model.

A mapping, defined in the framework of the Marumori–Yamamura–Tokunaga (MYT) boson expansion [13], from a 'physical' boson space onto a 'model' boson space, was proposed in [14] to describe multi-phonon processes. The same kind of mapping was used in [15] to study the Lipkin model expressed in the Schwinger realization of the $su(2)$ algebra. In particular, a multi-boson coherent state suitable to be used as a trial function in the time-dependent variational method was introduced. The new coherent state has the form of the extended coherent states discussed in [16].

In [17], the ground-state energy and the time evolution of large amplitude collective motion of the Lipkin model have been investigated in the framework of generalized coherent states. In the present paper we test the Glauber coherent state and its projections on subspaces characterized by specific eigenvalues of conserved observables, focusing on the groundstate, first excited state and the so-called random phase approximation (RPA) energies. In the mean-field approximation this model exhibits a second-order phase transition from a weak-coupling regime to a strong-coupling regime. We find that the trial states considered, especially the variational states defined in the eigenspace of the Casimir operator, in consonance with the parity symmetry of the model, reproduce very well the behaviour of the transition region from the weak to the strong coupling regimes.

The ground-state energy of the Lipkin model was recently obtained by Tsue, Azuma, Kuriyama and Yamamura only by use of the quasi-spin coherent sate [18].

2. The Lipkin model and the Schwinger realization of the $su(2)$ algebra

We consider the Lipkin model, equivalently defined by the Hamiltonian

$$H = T_0 + g\left(T_+^2 + T_-^2\right), \tag{1}$$

where T_0, T_+, T_- are generators of the $su(2)$ algebra and the coupling constant g is real and positive. In terms of boson operators $a^\dagger$, a, $b^\dagger$, b, obeying the relations $[a, a^\dagger] = [b, b^\dagger] = 1$, $[a, b^\dagger] = [b, a^\dagger] = [a, b] = [b^\dagger, a^\dagger] = 0$, the following representation, the so-called Schwinger realization of the $su(2)$ algebra, holds:

$$T_0 = \tfrac{1}{2}(a^\dagger a - b^\dagger b), \qquad T_+ = a^\dagger b, \qquad T_- = b^\dagger a.$$

The operator

$$C = \tfrac{1}{2}(a^\dagger a + b^\dagger b)$$

commutes with all the elements of the algebra. It plays the role of the Casimir operator, to which it is obviously related. Its eigenvalues Ω represent half the value of the common degeneracy of the lower and upper levels, and of the number of fermions in the model. The Schwinger realization of the Lipkin model is considered in the following development.

2.1. Glauber coherent state

The Glauber coherent state may be expressed as

$$|\Phi_G\rangle = \exp(\mu a^\dagger + \nu b^\dagger)|0\rangle. \tag{2}$$

Then we have

$$\langle\Phi_G|\Phi_G\rangle = \exp(|\mu|^2 + |\nu|^2),$$
$$\langle\Phi_G|T_0|\Phi_G\rangle = \tfrac{1}{2}(|\mu|^2 - |\nu|^2)\langle\Phi_G|\Phi_G\rangle,$$
$$\langle\Phi_G|T_+^2 + T_-^2|\Phi_G\rangle = (\mu^{*2}\nu^2 + \nu^{*2}\mu^2)\langle\Phi_G|\Phi_G\rangle.$$

Minimization of the expectation value of the Hamiltonian

$$\mathcal{H} = \frac{\langle\Phi_G|H|\Phi_G\rangle}{\langle\Phi_G|\Phi_G\rangle} = \frac{1}{2}(|\mu|^2 - |\nu|^2) + g((\mu^*\nu)^2 + (\nu^*\mu)^2)$$

under the constraint

$$\frac{\langle\Phi_G|a^\dagger a + b^\dagger b|\Phi_G\rangle}{\langle\Phi_G|\Phi_G\rangle} = \mu^*\mu + \nu^*\nu = 2\Omega,$$

which amounts to imposing average conservation of the Casimir operator, yields $\mathcal{H}_{\min} = -\Omega$ for $g \leqslant 1/(4\Omega)$, $\mathcal{H}_{\min} = -(16g^2\Omega^2 + 1)/(8g)$ for $g \geqslant 1/(4\Omega)$. We remark that in the deformed region the minimum is degenerated, i.e., if μ_0, ν_0 minimizes $\mathcal{H}$, so does $-\mu_0$, ν_0. This means that the potential energy has a double minimum, which is the source of the tunnel effect investigated in [8].

It is well known that the time evolution of an arbitrary quantal wave packet $|c\rangle$ is determined by the following variational principle [3]:

$$\delta \int_{t_1}^{t_2} L \,\mathrm{d}t = 0, \tag{3}$$

$$L = \mathrm{i}\langle c|\frac{\mathrm{d}}{\mathrm{d}t}|c\rangle - \langle c|H|c\rangle, \tag{4}$$

where H denotes the Hamiltonian operator of the system under consideration. For a system of fermions, $|c\rangle$ may be approximated by a Slater determinant and then (3) and (4) lead to the familiar TDHF equations [3]. The so-called Berry phase is nothing else than the first term on the right hand side of equation (4), $B = \mathrm{i}\langle c|\mathrm{d}/\mathrm{d}t|c\rangle$.

If we approximately restrict the dynamics of our system, namely the Lipkin model, to a Glauber coherent state (2), by an easy computation we easily find that the corresponding Berry phase reads

$$\mathcal{B} = -\frac{\langle\Phi_G|\dot{\Phi}_G\rangle - \langle\dot{\Phi}_G|\Phi_G\rangle}{2\mathrm{i}\langle\Phi_G|\Phi_G\rangle} = -\frac{1}{2\mathrm{i}}(\mu^*\dot{\mu} - \dot{\mu}^*\mu + \nu^*\dot{\nu} - \dot{\nu}^*\nu).$$

It is clear that the previous result involves taking correctly into account the lack of normalization of the state (2). A total derivative without consequences has also been neglected.

For $\theta = 2(\arg\mu - \arg\nu)$ and $|\mu^2| + |\nu|^2 = 2\Omega$, the Lagrangian, in the deformed region, reduces to

$$\mathcal{L} = -\tfrac{1}{2}\dot{\theta}|\mu|^2 - |\mu|^2 - 2g|\mu|^2(2\Omega - |\mu|^2)\cos\theta,$$

which allows us to easily obtain the RPA frequency

$$\omega = \sqrt{2(16g^2\Omega^2 - 1)} \qquad \text{for} \quad g \geqslant \frac{1}{4\Omega}.$$

In the non-deformed region, the dynamics is conveniently described by the quadratic Lagrangian

$$\mathcal{L}^{(2)} = -\frac{1}{2\mathrm{i}}(\dot{\gamma}\gamma^* - \gamma\dot{\gamma}^*) - 2\gamma\gamma^* - 4g\Omega\sqrt{\gamma\gamma^*}(\gamma + \gamma^*), \tag{5}$$

where, $|\gamma| = |\mu|/\sqrt{2}$, $\arg\gamma = 2(\arg\mu - \arg\nu)$. This leads to the RPA frequency

$$\omega = 2\sqrt{1 - 16g^2\Omega^2} \qquad \text{for} \quad g \leqslant \frac{1}{4\Omega}.$$

In this connection, we wish to observe that the quadratic Lagrangian (5) is not completely free from ambiguity. An alternative choice with $\arg\gamma = (\arg\mu - \arg\nu)$ is possible, which would lead to an RPA frequency with half the previous value.

3. Projection of Glauber coherent states

As it has been observed in the introduction, the Lipkin Model has been used to test the HF and TDHF theories [3] among others. This means describing a many-fermion system by a Slater determinant (SD) $|\Phi\rangle$ which may be related to a reference SD $|\Phi_0\rangle$ through an expression of the form $|\Phi\rangle = \exp(S)|\Phi_0\rangle$, where S is an arbitrary one-body operator. In the case of the Lipkin model, $|\Phi_0\rangle$ is taken to be the many-fermion state with all lower level states occupied and all the upper level states empty, as described in section 1. Without loss of generality, S may be conveniently restricted to the form $S = \gamma T_+$. Thus, $|\Phi_0\rangle$ satisfies $T_-|\Phi_0\rangle = 0$, $T_0|\Phi_0\rangle = -\Omega|\Phi_0\rangle$. In our boson realization we have $|\Phi_0\rangle = b^{\dagger 2\Omega}|0\rangle$.

The Glauber coherent state (2) is not an eigenstate of the relevant constants of motion. To compensate for this disadvantage, we are led to consider the projection of the Glauber coherent state on the eigenspace of the Casimir operator. SD $|\Phi\rangle$, or more precisely its boson image, is nothing else than that projection. Neglecting the normalization, we may also write

$$|\Phi\rangle = (\mu a^\dagger + \nu b^\dagger)^{2\Omega}|0\rangle \tag{6}$$

for the projection of $|\Phi_G\rangle$ on the eigenspace of the Casimir operator specified by the quantum number Ω. Then, the expectation value of the Hamiltonian reads

$$\mathcal{H} = \frac{\langle\Phi|H|\Phi\rangle}{\langle\Phi|\Phi\rangle} = \Omega\frac{\mu^*\mu - \nu^*\nu}{\mu^*\mu + \nu^*\nu} + g2\Omega(2\Omega - 1)\frac{\mu^{*2}\nu^2 + \nu^{*2}\mu^2}{(\mu^*\mu + \nu^*\nu)^2},$$

and the corresponding Berry phase reads

$$\mathcal{B} = -\frac{\langle\Phi|\dot{\Phi}\rangle - \langle\dot{\Phi}|\Phi\rangle}{2\mathrm{i}\langle\Phi|\Phi\rangle} = -2\Omega\frac{\mu^*\dot{\mu} + \nu^*\dot{\nu} - \dot{\mu}^*\mu - \dot{\nu}^*\nu}{2\mathrm{i}(\mu^*\mu + \nu^*\nu)}.$$

Minimization of $\mathcal{H}$ yields $\mathcal{H}_{\min} = -\Omega$ for $g \leqslant 1/(4\Omega - 2)$, $\mathcal{H}_{\min} = -\Omega(4g^2(2\Omega - 1)^2 + 1)/(8g\Omega - 4g)$ for $g \geqslant 1/(4\Omega - 2)$. We remark that, again, in the deformed region the minimum is degenerate, i.e., if μ_0, ν_0 minimizes $\mathcal{H}$, so does $-\mu_0$, ν_0. This means that, again, the potential energy has a double minimum.

For $p = (\mu^*\mu - \nu^*\nu)/(\mu^*\mu + \nu^*\nu)$, $\theta = \arg\mu - \arg\nu$, we get

$$\mathcal{H} = \Omega p + \Omega(2\Omega - 1)g(1 - p^2)\cos 2\theta, \qquad \mathcal{B} = -\Omega p\dot{\theta}.$$

We remark that, since $-1 \leqslant p \leqslant 1$, this parametrization is useful only in the deformed region, where Ωp, θ are canonically conjugate variables. The RPA frequency is

$$\omega = \sqrt{2(4(2\Omega - 1)^2 g^2 - 1)} \qquad \text{for} \quad g \geqslant \frac{1}{2(2\Omega - 1)}.$$

In the non-deformed region ($g \leqslant 1/(4\Omega - 2)$), the dynamics is described by the quadratic Lagrangian

$$\mathcal{L}^{(2)} = \frac{\mathrm{i}}{2}(\dot{\gamma}\gamma^* - \gamma\dot{\gamma}^*) - 2\gamma\gamma^* - 2g(2\Omega - 1)\sqrt{\gamma\gamma^*}(\gamma + \gamma^*), \tag{7}$$

where $|\gamma| = \sqrt{\Omega}|\mu/\nu|$, $\arg\gamma = 2(\arg\mu - \arg\nu)$. The RPA frequency reads

$$\omega = 2\sqrt{1 - 4(2\Omega - 1)^2 g^2} \qquad \text{for} \quad g \leqslant \frac{1}{2(2\Omega - 1)}.$$

In this connection, we wish to observe that the quadratic Lagrangian (7) is not completely free from ambiguity. An alternative choice with $\arg\gamma = (\arg\mu - \arg\nu)$ is possible, which would lead to an RPA frequency with half the previous value. The main change associated with the replacement of $|\Phi_G\rangle$ by its projection $|\Phi\rangle$ has been the replacement of the dimensionless effective coupling constant $\chi = 4g\Omega$ by a new coupling constant $\chi' = 2(2\Omega - 1)g$ in the expressions for the groundstate and RPA energies.

4. Even–even and odd–odd invariant subspaces

For simplicity, we restrict our discussion to the case of Ω being an integer. The case of Ω being a half-integer is treated similarly. From the parity symmetry of the Hamiltonian H, equation (1), it follows that it remains invariant under the canonical transformation $a \to a$, $b \to -b$. From this invariance, it is seen that the subspaces spanned by the kets

$$|\zeta_e(p,q)\rangle = \frac{1}{\sqrt{(2p)!(2q)!}}a^{\dagger 2p}b^{\dagger 2q}|0\rangle, \quad \text{with} \quad p + q = \Omega, \tag{8}$$

and by the kets

$$|\zeta_o(p,q)\rangle = \frac{1}{\sqrt{(2p+1)!(2q+1)!}}a^{\dagger(2p+1)}b^{\dagger(2q+1)}|0\rangle, \quad \text{with} \quad p + q = \Omega - 1, \tag{9}$$

are separately left invariant by H. This invariance is the source of the tunnel effect investigated in [8, 19] and the origin of the double minimum in the potential energy which has been mentioned before. In order to thoroughly evaluate its effect we are led to consider the projections of our trial state on the invariant subspaces with even–even (8) and odd–odd (9) boson numbers. The projection of $|\Phi\rangle$, equation (6), on the even–even subspace reads

$$|\Phi_e\rangle = 2\sum_{p,q}\frac{\mu^{2p}\nu^{2q}a^{\dagger 2p}b^{\dagger 2q}}{(2p)!(2q)!}|0\rangle, \tag{10}$$

with $p+q=\Omega$. The projection of $|\Phi\rangle$ on the odd–odd subspace reads

$$|\Phi_o\rangle = 2\sum_{p,q}\frac{\mu^{2p+1}\nu^{2q+1}a^{\dagger(2p+1)}b^{\dagger(2q+1)}}{(2p+1)!(2q+1)!}|0\rangle, \tag{11}$$

with $p+q=\Omega-1$. Let

$$|\Phi_+\rangle = (\mu a^\dagger + \nu b^\dagger)^{2\Omega}|0\rangle, \qquad |\Phi_-\rangle = (\mu a^\dagger - \nu b^\dagger)^{2\Omega}|0\rangle.$$

Then

$$|\Phi_e\rangle = |\Phi_+\rangle + |\Phi_-\rangle, \qquad |\Phi_o\rangle = |\Phi_+\rangle - |\Phi_-\rangle.$$

For the even–even sector, the expectation value of the Hamiltonian reads

$$\begin{aligned}\mathcal{H}_e = \frac{\langle\Phi_e|H|\Phi_e\rangle}{\langle\Phi_e|\Phi_e\rangle} &= \Omega\mu^*\mu\frac{(\mu^*\mu+\nu^*\nu)^{2\Omega-1}+(\mu^*\mu-\nu^*\nu)^{2\Omega-1}}{(\mu^*\mu+\nu^*\nu)^{2\Omega}+(\mu^*\mu-\nu^*\nu)^{2\Omega}}\\ &\quad-\Omega\nu^*\nu\frac{(\mu^*\mu+\nu^*\nu)^{2\Omega-1}-(\mu^*\mu-\nu^*\nu)^{2\Omega-1}}{(\mu^*\mu+\nu^*\nu)^{2\Omega}+(\mu^*\mu-\nu^*\nu)^{2\Omega}}+2\Omega(2\Omega-1)g\\ &\quad\times\frac{(\mu^{*2}\nu^2+\nu^{*2}\mu^2)((\mu^*\mu+\nu^*\nu)^{2\Omega-2}+(\mu^*\mu-\nu^*\nu)^{2\Omega-2})}{(\mu^*\mu+\nu^*\nu)^{2\Omega}+(\mu^*\mu-\nu^*\nu)^{2\Omega}},\end{aligned}$$

and the corresponding Berry phase reads

$$\begin{aligned}\mathcal{B}_e &= -\frac{\langle\Phi_e|\dot\Phi_e\rangle-\langle\dot\Phi_e|\Phi_e\rangle}{2\mathrm{i}\langle\Phi_e|\Phi_e\rangle} = -2\Omega\\ &\times\frac{(\mu^*\dot\mu+\nu^*\dot\nu-\dot\mu^*\mu-\dot\nu^*\nu)(\mu^*\mu+\nu^*\nu)^{2\Omega-1}+(\mu^*\dot\mu-\nu^*\dot\nu-\dot\mu^*\mu+\dot\nu^*\nu)(\mu^*\mu-\nu^*\nu)^{2\Omega-1}}{2\mathrm{i}((\mu^*\mu+\nu^*\nu)^{2\Omega}+(\mu^*\mu-\nu^*\nu)^{2\Omega})}.\end{aligned}$$

For the odd–odd sector, similar expressions hold for the expectation value of the Hamiltonian

$$\mathcal{H}_o = \frac{\langle\Phi_o|H|\Phi_o\rangle}{\langle\Phi_o|\Phi_o\rangle} \tag{12}$$

and for the corresponding Berry phase

$$\mathcal{B}_o = -\frac{\langle\Phi_o|\dot\Phi_o\rangle-\langle\dot\Phi_o|\Phi_o\rangle}{2\mathrm{i}\langle\Phi_o|\Phi_o\rangle}. \tag{13}$$

They are presented in the appendix. The dependence of $\mathcal{H}_e, \mathcal{B}_e, \mathcal{H}_o$ and $\mathcal{B}_o$ on the angles $\phi = \arg\mu, \psi = \arg\nu$ is very simple. In $\mathcal{H}_e$ and $\mathcal{H}_o$ only the factor $(\mu^{*2}\nu^2+\nu^{*2}\mu^2) = 2|\mu|^2|\nu|^2\cos(2(\phi-\psi))$ is argument dependent. On the other hand, the Berry phases may be written as

$$\begin{aligned}\mathcal{B}_e &= -\Omega(\dot\phi-\dot\psi)\frac{(|\mu|^2-|\nu|^2)(|\mu|^2+|\nu|^2)^{2\Omega-1}+(|\mu|^2+|\nu|^2)(|\mu|^2-|\nu|^2)^{2\Omega-1}}{((|\mu|^2+|\nu|^2)^{2\Omega}+(|\mu|^2-|\nu|^2)^{2\Omega})}\\ \mathcal{B}_o &= -\Omega(\dot\phi-\dot\psi)\frac{(|\mu|^2-|\nu|^2)(|\mu|^2+|\nu|^2)^{2\Omega-1}-(|\mu|^2+|\nu|^2)(|\mu|^2-|\nu|^2)^{2\Omega-1}}{((|\mu|^2+|\nu|^2)^{2\Omega}-(|\mu|^2-|\nu|^2)^{2\Omega})}.\end{aligned}$$

In each one of the above expressions a term of the form $\Omega(\dot\phi+\dot\psi)/2$ has been omitted, since it does not contribute to the equations of motion. We are now able to obtain numerical results. The ground-state energy is estimated by the minimum of $\mathcal{H}_e$. The energy difference between the second excited state and the groundstate is estimated by the RPA frequency associated with $|\Phi_e\rangle$. The energy of the first excited state is estimated by the minimum of $\mathcal{H}_o$. The energy difference between the third and first excited states is estimated by the RPA frequency associated with $|\Phi_o\rangle$.

5. Marumori mapping

Following [14, 15], in this section we apply Marumori's approach [13] to obtain the boson representation of the dynamical variables of our system in terms of the relevant degrees of freedom. Already in [14, 15, 17], it has been shown that coherent states based on this approach incorporate important correlations of the model and tend to describe well the transition region. As we have remarked, the even–even subspace spanned by the kets (8) and the odd–odd subspace spanned by the kets (9) are separately left invariant by the Hamiltonian H, equation (1). We consider auxiliary bosons c_e, d_e and their vacuum $|0_e)$, and c_o, d_o and their vacuum $|0_o)$. The auxiliary Hilbert spaces are spanned by the normalized kets

$$|\zeta_e(p,q)) = \frac{1}{\sqrt{p!q!}} c_e^{\dagger p} d_e^{\dagger q} |0_e), \quad \text{with} \quad p+q=\Omega,$$
$$|\zeta_o(p,q)) = \frac{1}{\sqrt{p!q!}} c_o^{\dagger p} d_o^{\dagger q} |0_o), \quad \text{with} \quad p+q=\Omega-1.$$

We introduce the mappings

$$|\zeta_e(p,q)\rangle \to |\zeta_e(p,q)), \qquad |\zeta_o(p,q)\rangle \to |\zeta_o(p,q)).$$

Under these mappings, the boson images of the operators $a^{\dagger 2}, b^{\dagger 2}, a^\dagger a, b^\dagger b, \ldots$ are easily obtained. We find for the even–even subspace

$$a^{\dagger 2} \to \sqrt{2\big(2c_e^\dagger c_e - 1\big)}c_e^\dagger, \qquad b^{\dagger 2} \to \sqrt{2\big(2d_e^\dagger d_e - 1\big)}d_e^\dagger, \qquad a^\dagger a \to 2c_e^\dagger c_e, \qquad b^\dagger b \to 2d_e^\dagger d_e,$$

and for the odd–odd subspace

$$a^{\dagger 2} \to \sqrt{2\big(2c_o^\dagger c_o + 1\big)}c_o^\dagger, \quad b^{\dagger 2} \to \sqrt{2\big(2d_o^\dagger d_o + 1\big)}d_o^\dagger, \quad a^\dagger a \to 2c_o^\dagger c_o + 1, \quad b^\dagger b \to 2d_o^\dagger d_o + 1.$$

The boson images of the Hamiltonian H and of the state vectors may be easily obtained, if desired.

5.1. Trial state motivated by the Marumori mapping

We consider trial states which are motivated by the Marumori mapping. For the even–even sector, we take

$$|\Psi_e\rangle = \sum_{p,q,(p+q=\Omega)} \frac{\mu^p \nu^q a^{\dagger 2p} b^{\dagger 2q}}{p!q!\sqrt{1\cdot 3\cdot \ldots \cdot (2p-1)1\cdot 3\cdot \ldots \cdot (2q-1)}}|0\rangle. \tag{14}$$

Under the Marumori mapping, this state vector reduces to the ket $\big(\mu c_e^\dagger + \nu d_e^\dagger\big)^\Omega |0_e)$. This ket is the projection of a certain Glauber coherent state on a subspace with good eigenvalue of the Casimir operator, being that the motivation behind the present choice. The expectation value of the Hamiltonian,

$$\widetilde{\mathcal{H}}_e = \frac{\langle\Psi_e|H|\Psi_e\rangle}{\langle\Psi_e|\Psi_e\rangle},$$

is readily expressed in terms of the quantities

$$\langle\Psi_e|\Psi_e\rangle = \frac{2^\Omega}{\Omega!}(|\mu|^2+|\nu|^2)^\Omega,$$
$$\langle\Psi_e|T_0|\Psi_e\rangle = \Omega\frac{|\mu|^2-|\nu|^2}{|\mu|^2+|\nu|^2}\langle\Psi_e|\Psi_e\rangle,$$
$$\langle\Psi_e|T_+^2+T_-^2|\Psi_e\rangle = 2\cdot 2^{\Omega+1}\cos(\phi-\psi)\frac{|\nu|}{|\mu|}\sum_{p,q,(p+q=\Omega)}\frac{|\mu|^{2p}|\nu|^{2q}\sqrt{(2p-1)(2q+1)}}{(p-1)!q!},$$

where $\phi = \arg\mu$, $\psi = \arg\nu$. The corresponding Berry phase reads

$$\widetilde{\mathcal{B}}_e = -\frac{\Omega}{2}\left(\frac{|\mu|^2 - |\nu|^2}{|\mu|^2 + |\nu|^2}(\dot{\phi} - \dot{\psi}) + (\dot{\phi} + \dot{\psi})\right).$$

For the odd–odd sector we take, with $\Omega_o = \Omega - 1$,

$$|\Psi_o\rangle = \sum_{p,q,(p+q=\Omega_o)} \frac{\mu^p \nu^q a^{\dagger(2p+1)} b^{\dagger(2q+1)}}{p!q!\sqrt{3\cdot 5\cdot \ldots \cdot (2p+1)3\cdot 5\cdot \ldots \cdot (2q+1)}}|0\rangle. \tag{15}$$

Under the Marumori mapping, this state reduces to a very simple expression, namely the ket $\left(\mu c_o^\dagger + \nu d_o^\dagger\right)^{\Omega_o}|0_o\rangle$. The expectation value of the Hamiltonian,

$$\tilde{\mathcal{H}}_o = \frac{\langle\Psi_o|H|\Psi_o\rangle}{\langle\Psi_o|\Psi_o\rangle},$$

is readily expressed in terms of the quantities

$$\langle\Psi_o|\Psi_o\rangle = \frac{2^{\Omega_o}}{\Omega_o!}(|\mu|^2 + |\nu|^2)^{\Omega_o},$$

$$\langle\Psi_o|T_0|\Psi_o\rangle = \Omega_o\frac{|\mu|^2 - |\nu|^2}{|\mu|^2 + |\nu|^2}\langle\Psi_o|\Psi_o\rangle,$$

$$\langle\Psi_o|T_+^2 + T_-^2|\Psi_o\rangle = 2\cdot 2^{\Omega_o+1}\cos(\phi - \psi)\frac{|\nu|}{|\mu|}\sum_{p,q,(p+q=\Omega_o)}\frac{|\mu|^{2p}|\nu|^{2q}\sqrt{(2p+1)(2q+3)}}{(p-1)!q!}.$$

The corresponding Berry phase reads

$$\widetilde{\mathcal{B}}_o = -\frac{\Omega_o}{2}\left(\frac{|\mu|^2 - |\nu|^2}{|\mu|^2 + |\nu|^2}(\dot{\phi} - \dot{\psi}) + (\dot{\phi} + \dot{\psi})\right).$$

The appropriate Lagrangians may be easily found. We are now able to obtain numerical results. The ground-state energy is estimated by the minimum of $\tilde{\mathcal{H}}_e$. The energy difference between the second excited state and the groundstate is estimated by the RPA frequency associated with $|\Psi_e\rangle$. The energy of the first excited state is estimated by the minimum of $\tilde{\mathcal{H}}_o$. The energy difference between the third and first excited states is estimated by the RPA frequency associated with $|\Psi_o\rangle$.

6. Results and conclusions

In order to compare, in a variational sense, the performance of Glauber coherent states and some related state vectors, we have computed the groundstate and excitation energies of the system using those state vectors as trial functions. For different values of the coupling constant $\chi = 4g\Omega$, and for $\Omega = 6$, we compare, in figure 2, the exact ground-state energy with the lowest energy obtained with four types of trial states, namely, $|\Phi_G\rangle$, $|\Phi\rangle$, $|\Phi_e\rangle$ and $|\Psi_e\rangle$ (equations (2), (6), (10) and (14)). In figure 3, we compare the exact energy of the first excited state with the lowest energy obtained with two variants of trial states, namely, $|\Phi_o\rangle$ and $|\Psi_o\rangle$ (equations (11) and (15)). In figure 4, we compare the exact energy difference between the second excited state and the groundstate with the RPA energy obtained with the help of the trial states $|\Phi_G\rangle$, $|\Phi\rangle$, $|\Phi_e\rangle$ and $|\Psi_e\rangle$. Indeed, figure 1 suggests that the RPA frequency should be identified with the energy difference between the second excited state and the groundstate, at least in the deformed region, since the energy difference between the first excited state and the groundstate is precisely the level splitting associated with a tunnel effect [8]. In figure 5, we compare the exact energy difference between the third and the first

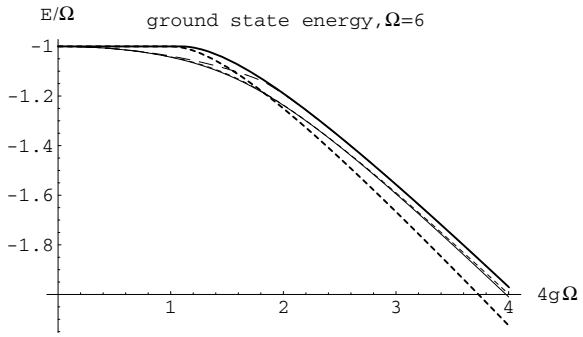

Figure 2. The thin continuous line shows the exact result (ground-state energy). The thick short-dashed line shows the Glauber state result. The thick continuous line corresponds to the projection $|\Phi\rangle$. The long-dashed line corresponds to the projection $|\Phi_e\rangle$. For large enough g, the curves corresponding to the projections $|\Phi\rangle$ and $|\Phi_e\rangle$, seem to merge into a single one. The result for the improved state $|\Psi_e\rangle$ is very close to the exact one and corresponds to the thin short-dashed line.

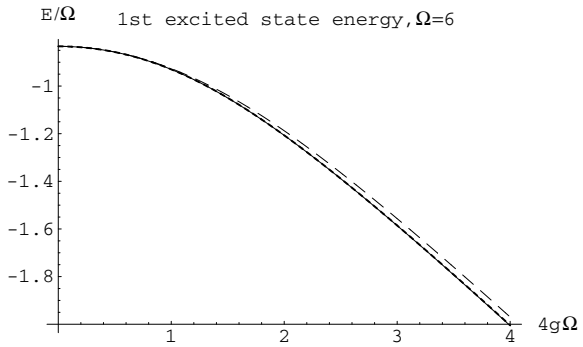

Figure 3. The thin continuous line shows the exact result (first excited state energy). The long-dashed line corresponds to the projection $|\Phi_o\rangle$. The result for the improved state $|\Psi_o\rangle$ almost coincides with the exact one and is shown by the thick short-dashed line.

excited states with the RPA energy obtained with the help of the trial states $|\Phi_o\rangle$ and $|\Psi_o\rangle$. The first conclusion to be drawn is that the Glauber coherent state $|\Phi_G\rangle$, (equation (2)), which is not an eigenstate of the Casimir operator, gives results which, not being the best ones, are, already, qualitatively acceptable. The Casimir operator is only conserved in the average by this state. It is clearly seen from figure 2 that the Glauber coherent state leads, for large values of the coupling constant, to energy values lying below the exact ground-state energy. This is not surprising, since this state contains components outside the physical subspace, characterized by a specific eigenvalue of the Casimir operator, and some of the eigenvalues of the hamiltonian H, equation (1), extended to the full Hilbert space lie below the lowest eigenvalue associated with the physical subspace. It should be said, however, that $|\Phi_G\rangle$ is quite reasonable up to the transition region and above that region, but not so good around it. Moreover, the performance of $|\Phi_G\rangle$ becomes increasingly better as Ω, the eigenvalue of the Casimir operator, is gradually increased. We will discuss more thoroughly the performance of conserving states which are eigenstates of the Casimir operator, namely $|\Phi\rangle$, $|\Phi_e\rangle$, $|\Phi_o\rangle$, $|\Psi_e\rangle$ and $|\Psi_o\rangle$, (equations (6), (10), (11), (14) and (15)). Several conclusions may be drawn as follows:

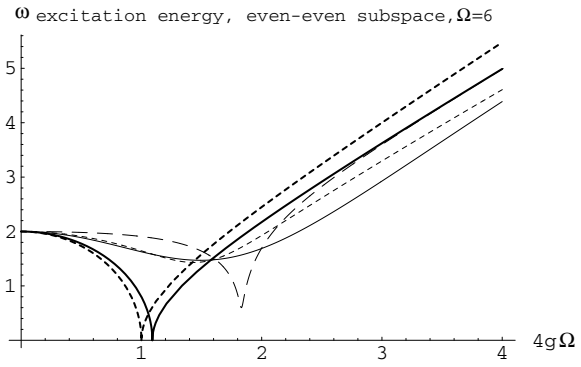

Figure 4. RPA frequencies (excitation energies). The thin continuous line shows the exact result (difference between second excited state and ground-state energies). The thick short-dashed line shows the Glauber state result. The thick continuous line corresponds to the projection $|\Phi\rangle$. The long-dashed line corresponds to the projection $|\Phi_e\rangle$. The result for the improved state $|\Psi_e\rangle$, shown by the thin-dashed line, is very close to the exact one.

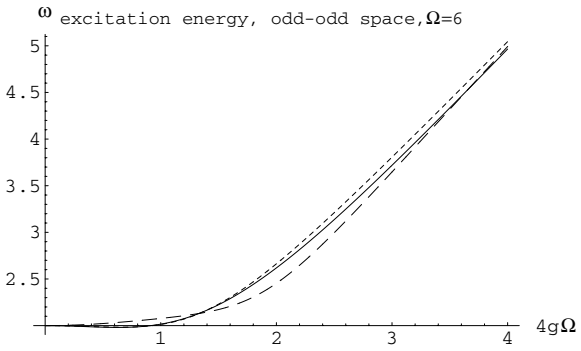

Figure 5. RPA frequencies (excitation energies). The thin continuous line shows the exact result (difference between third and first excited state energies). The long-dashed line corresponds to the projection $|\Phi_o\rangle$. The result for the improved state $|\Psi_o\rangle$, shown by the thick short-dashed line, is very close to the exact one.

- A slight improvement of the description of the ground-state energy is obtained when the Glauber coherent state $|\Phi_G\rangle$ is replaced by its projection $|\Phi\rangle$ on the eigenspace of the Casimir operator characterized by the eigenvalue Ω. However, the RPA frequency is still poorly described, especially in the transition region. The bad performance of $|\Phi_G\rangle$ and $|\Phi\rangle$ around the transition region is a manifestation of the well-known fact that quantum fluctuations are there very large and play an important role.
- The projection $|\Phi_e\rangle$ of $|\Phi\rangle$ on the invariant even–even subspace provides an improved description of the ground-state energy. The RPA associated with $|\Phi_e\rangle$ provides also an improved description of the excitation energy, understood as the energy difference between the second excited state and the groundstate.
- The projection $|\Phi_o\rangle$ of $|\Phi\rangle$ on the invariant odd–odd subspace provides a good description of the energy of the first excited state. The RPA associated with $|\Phi_o\rangle$ provides also a good description of the energy difference between the third and the first excited states.

- Next we have considered trial states which have, as their images under the Marumori mapping, projections of certain Glauber coherent states with good eigenvalues of the Casimir operator. The state $|\Psi_e\rangle$, belonging to the even–even subspace, provides an excellent description of the ground-state energy. The RPA associated with $|\Psi_e\rangle$ provides also an excellent description of the energy difference between the second excited state and the ground-state. It is remarkable that quantum fluctuations which are very large and play an important role around the transition region, are well described by the ket $|\Psi_e\rangle$.
- The state $|\Psi_o\rangle$, belonging to the odd–odd invariant subspace, provides an excellent description of the energy of the first excited state. The RPA associated with $|\Psi_o\rangle$ provides also an excellent description of the energy difference between the third and the first excited states.

In the present work we have verified that generalized coherent states defined in consonance with the parity symmetry of the model describe particularly well the transition from weak to strong coupling. In order to extend the method to more realistic situations we should first test its strength in describing a transition to a deformed phase with a broken continuous symmetry. A possible candidate is the $su(3)$ Lipkin model which has been recently studied within several approximations [20–23].

Acknowledgments

This work was supported by the Portuguese FCT through the Project POCI/FP/FNN/63419/2005.

Appendix

For the odd–odd sector, the expectation value of the Hamiltonian reads

$$\begin{aligned}\mathcal{H}_o = \frac{\langle\Phi_o|H|\Phi_o\rangle}{\langle\Phi_o|\Phi_o\rangle} &= \Omega\mu^*\mu\frac{(\mu^*\mu+\nu^*\nu)^{2\Omega-1}-(\mu^*\mu-\nu^*\nu)^{2\Omega-1}}{(\mu^*\mu+\nu^*\nu)^{2\Omega}-(\mu^*\mu-\nu^*\nu)^{2\Omega}}\\ &\quad-\Omega\nu^*\nu\frac{(\mu^*\mu+\nu^*\nu)^{2\Omega-1}+(\mu^*\mu-\nu^*\nu)^{2\Omega-1}}{(\mu^*\mu+\nu^*\nu)^{2\Omega}-(\mu^*\mu-\nu^*\nu)^{2\Omega}}\\ &\quad+2\Omega(2\Omega-1)g\frac{(\mu^{*2}\nu^2+\nu^{*2}\mu^2)((\mu^*\mu+\nu^*\nu)^{2\Omega-2}-(\mu^*\mu-\nu^*\nu)^{2\Omega-2})}{(\mu^*\mu+\nu^*\nu)^{2\Omega}-(\mu^*\mu-\nu^*\nu)^{2\Omega}},\end{aligned}$$

and the Berry phase reads

$$\begin{aligned}\mathcal{B}_o &= -\frac{\langle\Phi_o|\dot\Phi_o\rangle-\langle\dot\Phi_o|\Phi_o\rangle}{2\mathrm{i}\langle\Phi_o|\Phi_o\rangle}=-2\Omega\\ &\times\frac{(\mu^*\dot\mu+\nu^*\dot\nu-\dot\mu^*\mu-\dot\nu^*\nu)(\mu^*\mu+\nu^*\nu)^{2\Omega-1}-(\mu^*\dot\mu-\nu^*\dot\nu-\dot\mu^*\mu+\dot\nu^*\nu)(\mu^*\mu-\nu^*\nu)^{2\Omega-1}}{2\mathrm{i}((\mu^*\mu+\nu^*\nu)^{2\Omega}-(\mu^*\mu-\nu^*\nu)^{2\Omega})}.\end{aligned}$$

References

[1] Lipkin H J, Meshkov N and Glick A 1965 *Nucl. Phys.* **62** 188
Lipkin H J, Meshkov N and Glick A 1965 *Nucl. Phys.* **62** 211
[2] Kan K K, Lichtner P C, Dworczeka M and Griffin J J 1980 *Phys. Rev.* C **21** 1098
[3] Yamamura M and Kuriyama K 1987 *Prog. Theor. Phys. Suppl.* **93** 1–176
[4] Holzwarth G 1997 *Nucl. Phys.* A **207** 545
[5] Pang S C, Klein A and Dreizler R M 1968 *Ann. Phys., NY* **49** 477
[6] Ring P and Schuck P 1980 *The Nuclear Many-Body Problem* (New York: Springer)

[7] Botet R, Jullien R and Pfeuty P 1982 *Phys. Rev. Lett.* **49** 478
[8] Belinicher V J, Providência C and da Providência J 1997 *J. Phys. A: Math. Gen.* **30** 5633
[9] Cirac J I, Lewenstein M, Mœlmer K and Zoller P 1998 *Phys. Rev.* A **57** 1208
[10] Vidal J, Palacios G and Mosseri R 2004 *Phys. Rev.* A **69** 022107
[11] Heiss W D 2006 *J. Phys. A: Math. Gen.* **39** 10081
[12] Klein A and Marshalek E R 1991 *Rev. Mod. Phys.* **63** 375
[13] Marumori T, Yamamura M and Tokunaga A 1964 *Prog. Theor. Phys.* **31** 1009
[14] Kuriyama A, Providência C, da Providência J, Tsue Y and Yamamura M 2001 *Prog. Theor. Phys.* **106** 751
[15] Kuriyama A, Providência C, da Providência J and Yamamura M 2000 *Prog. Theor. Phys.* **103** 733
[16] Kuriyama A, da Providência J, Tsue Y and Yamamura M 1997 *Prog. Theor. Phys.* **98** 381
[17] Kuriyama A, Yamamura M, Providência C and da Providência J 2003 *J. Phys. A: Math. Gen.* **36** 10361
[18] Tsue Y, Azuma N, Kuriyama A and Yamamura M 1996 *Prog. Theor. Phys.* **96** 729
[19] Nishiyama S, Ido M and Ishida K 1998 *Int. J. Mod. Phys.* E **8** 443
[20] Brito L, Providência C, da Providência J, Avancini S S, de Souza Cruz F F, Menezes D P and Watanabe Moraes M M 1995 *Phys. Rev.* A **52** 92
[21] Hagino K and Bertsch G F 2000 *Phys. Rev.* C **61** 024307
[22] Delion D S, Schuck P and Dukelsky J 2005 *Phys. Rev.* C **72** 064305
[23] Providência C, da Providência J, Tsue Y and Yamamura M 2006 *Prog. Theor. Phys.* **115** 143
Providência C, da Providência J, Tsue Y and Yamamura M 2006 *Prog. Theor. Phys.* **115** 155